

PlotChain: Deterministic Checkpointed Evaluation of Multimodal LLMs on Engineering Plot Reading

Mayank Ravishankara

Independent Researcher, San Francisco, CA, USA

Email: mrvisha@alumni.cmu.edu (alt: mayankgowda@gmail.com)

Abstract—We present **PlotChain**, a deterministic, generator-based benchmark for evaluating multimodal large language models (MLLMs) on *engineering plot reading*—recovering quantitative values from classic plots (e.g., Bode/FFT, step response, stress-strain, pump curves) rather than OCR-only extraction or free-form captioning. PlotChain contains 15 plot families with 450 rendered plots (30 per family), where every item is produced from known parameters and paired with exact ground truth computed directly from the generating process. A central contribution is *checkpoint-based diagnostic evaluation*: in addition to final targets, each item includes intermediate “cp_” fields that isolate sub-skills (e.g., reading cutoff frequency or peak magnitude) and enable failure localization within a plot family. We evaluate four state-of-the-art MLLMs under a standardized, deterministic protocol (temperature = 0 and a strict JSON-only numeric output schema) and score predictions using per-field tolerances designed to reflect human plot-reading precision. Under the `plotread` tolerance policy, the top models achieve 80.42% (Gemini 2.5 Pro), 79.84% (GPT-4.1), and 78.21% (Claude Sonnet 4.5) overall field-level pass rates, while GPT-4o trails at 61.59%. Despite strong performance on many families, frequency-domain tasks remain brittle: bandpass response stays low ($\leq 23\%$), and FFT spectrum remains challenging. We release the generator, dataset, raw model outputs, scoring code, and manifests with checksums to support fully reproducible runs and retrospective rescoreing under alternative tolerance policies.

Index Terms—multimodal LLM, benchmark, plot understanding, chart reasoning, reproducibility, engineering plots

I. INTRODUCTION

Engineering practice is mediated by plots: Bode magnitude/phase curves, FFT spectra, step responses, stress–strain diagrams, IV curves, pump characteristic curves, and calibration charts are routinely used to validate designs, troubleshoot systems, and communicate quantitative results. Progress is difficult to measure without benchmarks that (i) target *engineering* plot families (not generic infographic charts), (ii) provide *exact* and auditable ground truth, and (iii) support *diagnostic* evaluation that distinguishes visual read errors from downstream arithmetic or reasoning errors.

Existing work on chart and figure understanding has made important advances, but typical benchmarks are not designed to isolate the specific failure modes that arise in engineering plot reading. Early datasets such as FigureQA provide synthetic scientific-style plots with template questions and auxiliary annotations [1]. DVQA focuses on bar charts and highlights brittleness to appearance variation and the challenge of answers unique to each chart [2]. PlotQA targets scientific plots at scale and emphasizes reasoning and out-of-vocabulary

numeric answers [3]. ChartQA introduces human-written questions that require visual and logical reasoning over charts, often leveraging the underlying chart data table [4]. More recent MLLM-focused suites (e.g., ChartBench) broaden chart types and question styles for chart comprehension evaluation [5], while general multimodal reasoning benchmarks (e.g., Math-Vista and MMMU) include charts among many heterogeneous modalities and tasks [6], [7]. These resources are valuable, yet they commonly (a) emphasize generic chart QA or captioning rather than canonical *engineering* plot families, (b) evaluate final answers without intermediate sub-skill probes, and/or (c) rely on data tables or human annotations in ways that make “ground truth” less directly attributable to the plotted rendering process [3], [4], [5].

In this paper, we introduce **PlotChain**, a deterministic, generator-based benchmark tailored to *engineering plot reading*. PlotChain renders plot images from known parameters and computes ground truth deterministically from those same parameters, enabling exact verification and eliminating annotation noise. The benchmark spans **15 plot families** with **450 items** (30 per family), with controlled difficulty settings (clean/moderate/edge) that remain human-readable but stress common plot-reading challenges such as sparse tick marks, reduced grid cues, tighter axis windows, and ambiguous intersections. Each item pairs a natural-language question with a required *strict JSON* numeric response schema to support automated scoring and reproducible evaluation.

A central novelty is *checkpoint-based diagnostic evaluation*. In addition to final target fields, items may include intermediate “cp_” fields that correspond to localized plot reads (e.g., reading a cutoff frequency, peak magnitude, intercept, slope region, or axis scale) that are scored separately from final fields. This design turns plot reading into a sequence of verifiable sub-reads, enabling fine-grained attribution: models may succeed at reading intermediate quantities yet fail on derived quantities (or vice versa), which is not observable from a single final-answer score. To reflect realistic human plot interpretation, we score numeric predictions using per-field tolerances (absolute and/or relative), rather than exact string match, and we report both headline pass rates and per-family diagnostic breakdowns.

Finally, reproducibility is treated as a first-class objective. Motivated by broader calls for transparent, reproducible ML evaluation [8], and benchmark practices that release prompts and raw outputs for auditability [9], PlotChain is distributed

with the generator, dataset JSONL, evaluation scripts, raw model outputs, and manifests with checksums and run metadata. This enables exact re-runs when possible and retrospective rescore under alternative tolerance or parsing policies without re-querying model APIs.

a) *Contributions*.:

- **Deterministic engineering-plot benchmark:** a generator-based dataset spanning 15 canonical engineering plot families with exact ground truth derived from generation parameters.
- **Checkpoint-based diagnostics:** intermediate “cp_*” fields that isolate plot-reading sub-skills and enable failure localization beyond final-answer evaluation.
- **Standardized, deterministic evaluation protocol:** uniform prompting and decoding controls (temperature = 0) with strict JSON numeric outputs, coupled with tolerance-based scoring aligned to human plot reading.
- **Reviewer-auditable artifact release:** code, data, raw outputs, and manifests with checksums to support reproducible runs and post-hoc analysis.

II. RELATED WORK

Interpreting engineering plots requires extracting quantitative values (often absent from the rendered pixels), mapping visual encodings to axes/units, and performing light numerical reasoning under perceptual uncertainty. Prior work spans (i) chart/plot question answering benchmarks, (ii) chart *derendering* and plot-to-table conversion, (iii) chart summarization/captioning for accessibility, and (iv) broader multimodal benchmarks and evaluation practices.

A. Chart and Plot Question Answering Benchmarks

Early work studied chart question answering alongside explanation generation, typically assuming access to structured chart specifications or focusing on smaller curated sets [10]. Synthetic benchmarks such as FigureQA [1] and DVQA [2] scaled supervision by programmatically generating charts and questions; these enabled controlled evaluation but often emphasize discrete labels or restricted answer forms and chart styles.

PlotQA [3] targets scientific plots with real-valued answers and larger variability, highlighting challenges beyond fixed vocabularies and prompting hybrid pipelines that combine perception with structured reasoning. ChartQA [4] extends to real-world charts (with human-written questions) and emphasizes both visual and logical reasoning, often relying on explicit table extraction or auxiliary parsing of chart elements. Collectively, these datasets demonstrate that chart understanding is neither pure OCR nor generic captioning, but a compositional perception–reasoning problem with brittle failure modes.

B. Derendering and Plot-to-Table Conversion

A complementary line of work treats charts as a structured graphics modality to be *derendered* into underlying data tables or symbolic representations. Earlier systems and interactive tools addressed chart data extraction as a core primitive for

downstream reasoning and accessibility [11], [12]. ChartOCR [13] combines learned and rule-based components and introduces large-scale annotated data for chart elements.

More recent approaches emphasize end-to-end or unified modeling. ChartReader [14] proposes a unified framework that supports both derendering and comprehension without heavy manual rule design. Pix2Struct [15] pretrains on screenshot-to-structured-output tasks and is frequently used as a strong baseline for chart/plot parsing. UniChart [16] introduces chart-specific pretraining objectives to improve both low-level extraction and high-level reasoning.

DePlot [17] popularizes a modality-conversion strategy: translate plots into a table-like representation and then perform reasoning on the structured output, while also discussing inconsistencies in evaluation metrics across chart types. Benchmarking studies on LVLM chart capability and correction strategies further document systematic chart-specific weaknesses and evaluation pitfalls [18].

C. Chart Summarization and Accessibility

Chart-to-text and summarization benchmarks focus on generating natural-language descriptions of charts, motivated by accessibility and visualization literacy [19], [20]. While these tasks overlap with plot understanding, they emphasize narrative faithfulness and content selection rather than numeric extraction accuracy under realistic plot-reading tolerances.

D. Chart-Focused Evaluation in the LVLM Era

With large vision-language models, several chart-focused evaluations and benchmarks have emerged to probe chart reasoning and robustness [5], [21]. These efforts reinforce the need for evaluation designs that separate (a) visual extraction from (b) reasoning, and that characterize failure modes beyond a single final-answer metric.

Broader multimodal benchmarks, including MMBench [22], MathVista [6], and MMMU [7], evaluate general multimodal understanding and reasoning, but are not designed specifically for quantitative engineering-style plot reading or for checkpoint-based diagnostic analysis. [23].

E. Benchmarking Methodology and Reproducibility

Standardized evaluation protocols and artifact release practices are increasingly emphasized in the language and multimodal model literature [9], [8]. Our work aligns with this direction by centering deterministic generation, checksummed artifacts, fixed decoding settings, and storing raw outputs to enable rescore under revised tolerance policies. We use standard scientific Python tooling commonly cited in reproducible ML pipelines [24], [25], [26].

III. BENCHMARK DESIGN AND DATASET

A. Task Definition

PlotChain evaluates *engineering plot reading* by multimodal LLMs: given an image of a canonical engineering plot and a natural-language question, the model must return a *single JSON object* whose values are numeric (or null when

TABLE I: PlotChain plot families and representative target variables (final fields; checkpoint fields are prefixed `cp_` and omitted for brevity).

Family	Domain / Axes	Representative final outputs
step_response	Controls; time vs response	percent_overshoot, settling_time_s, steady_state
bode_magnitude	Circuits/controls; log-f vs dB	dc_gain_db, cutoff_hz
bode_phase	Circuits/controls; log-f vs deg	cutoff_hz, phase_deg_at_fq
bandpass_response	Filters; log-f vs dB	resonance_hz, bandwidth_hz
time_waveform	Signals; time vs voltage	frequency_hz, vpp_v
fft_spectrum	Signals; f vs magnitude	dominant_frequency_hz, secondary_frequency_hz
spectrogram	Signals; time-freq heatmap	f1_hz, f2_hz, switch_time_s
iv_resistor	Circuits; V-I linear	resistance_ohm
iv_diode	Circuits; V-I exponential	target_current_a, turn_on_voltage_v_at_target_i
transfer_characteristic	Nonlinear blocks; V_{in} - V_{out}	small_signal_gain, saturation_v
pole_zero	Systems; complex plane	pole_real, pole_imag, zero_real, zero_imag
stress_strain	Materials; strain vs stress	yield_strength_mpa, uts_mpa, fracture_strain
torque_speed	Motors; speed vs torque	stall_torque_nm, no_load_speed_rpm
pump_curve	Fluids; flow vs head	head_at_qop_m, q_at_half_head_m3h
sn_curve	Fatigue; log-log cycles vs stress	stress_at_1e5_mpa, endurance_limit_mpa

explicitly instructed). Unlike OCR-only settings, PlotChain requires interpreting axes (including log scales), reading off curve values, and computing derived quantities consistent with standard engineering practice (e.g., cutoff frequency at -3 dB, settling time by a tolerance band, bandwidth between -3 dB points).

Each item specifies two categories of target fields:

- **Final fields** (headline): the main numeric answers (e.g., `cutoff_hz`, `settling_time_s`).
- **Checkpoint fields** (diagnostics): intermediate reads prefixed `cp_` (e.g., `cp_mag_at_fc_db`, `cp_peak_value`) that localize failure modes and enable stepwise capability analysis.

B. Plot Families

PlotChain contains 15 plot families (30 items per family; 450 total items). Table I summarizes families, domains, and representative outputs. Families are chosen to reflect common analysis patterns in controls, signals, circuits, mechanical systems, and materials.

C. Deterministic Generation and Ground Truth

All items are generated by a *frozen* generator that deterministically maps (`master_seed`, `family`, `index`) to: (i) plot parameters, (ii) a rendered PNG plot image, and (iii) a ground-truth dictionary computed directly from the generating parameters using explicit analytic / numeric baselines (not OCR). This design yields *verifiable gold labels*: for every numeric target, the paper can (and does) release the corresponding parameterization and baseline used to compute the value.

To maintain human-readability and avoid pathological targets (e.g., irrational or visually implausible fractions), PlotChain *quantizes* ground-truth values to family/field-specific decimal precision (e.g., integer Hz cutoffs, 0.1 dB gains, and task-appropriate rounding for times/ratios). This makes the evaluation reflect realistic plot reading rather than ultra-fine numerical reconstruction.

D. Difficulty and Edge-Case Design

Within each family, items follow an intended difficulty mixture of approximately **40% clean / 30% moderate / 30% edge**. **Clean** items include standard visual aids (ticks, gridlines, clear axis windows). **Moderate** items apply controlled perturbations (e.g., mild noise) while remaining readable. **Edge** items remove or weaken visual aids (e.g., tighter axis windows or reduced cues) but are constrained by a manual readability protocol to remain solvable by a human using approximate plot-reading.

E. Dataset Format and Released Artifacts

PlotChain is distributed as:

- a JSONL file (`plotchain.jsonl`) containing one object per item;
- per-family image directories (`images/<family>/...`.png);
- validation CSVs produced by the generator (row-level and summary-level sanity checks).

Each JSONL item includes:

- `id`, `type`, `image_path`, `question`;
- `ground_truth`: dictionary with both final fields and optional `cp_checkpoint` fields;
- `plot_params`: generating parameters required to reproduce the plot and recompute labels;
- `generation`: metadata including deterministic seed, difficulty tag, and explicit lists of final vs checkpoint fields.

IV. EXPERIMENTAL SETUP AND EVALUATION

A. Model Suite and Deterministic Decoding

We evaluate PlotChain using four state-of-practice multimodal LLMs spanning three providers: (i) OpenAI GPT-4.1, (ii) OpenAI GPT-4o, (iii) Anthropic Claude Sonnet 4.5, and (iv) Google Gemini 2.5 Pro. To maximize reproducibility, all evaluations use deterministic decoding (temperature = 0) with a shared prompt template and a fixed maximum output

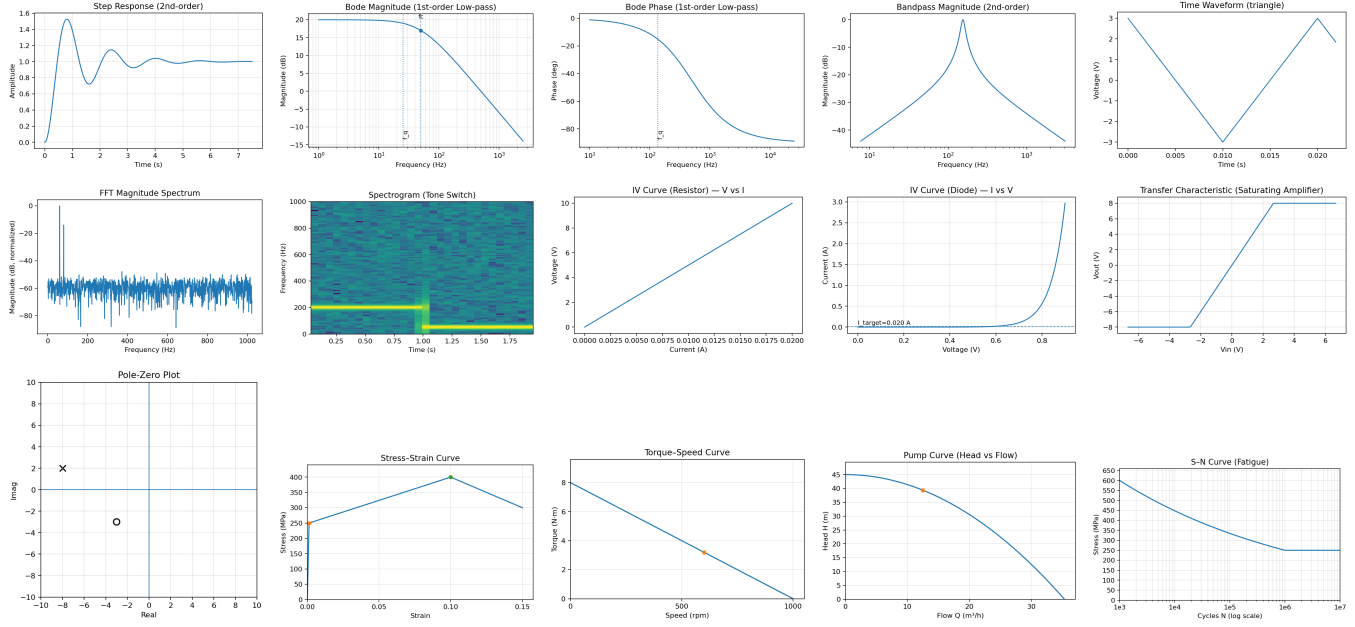


Fig. 1: Representative PlotChain samples (one per family). Row 1: Step response; Bode magnitude; Bode phase; Bandpass frequency response; Time-domain waveform. Row 2: FFT magnitude spectrum; Spectrogram; Resistor I–V curve; Diode I–V curve; Transfer characteristic. Row 3: Pole–zero plot; Stress–strain curve; Torque–speed curve; Pump characteristic curve; S–N fatigue curve.

TABLE II: Evaluated models and run configuration (Jan. 2026; temperature = 0 for all runs).

Provider	Model	Notes
OpenAI	GPT-4.1	Shared prompt; strict JSON-only numeric schema
OpenAI	GPT-4o	Same settings as above
Anthropic	Claude Sonnet 4.5	Same settings; multimodal (image+text) input
Google	Gemini 2.5 Pro	Same settings; fixed high token budget in our implementation

token budget. Run timestamps, model identifiers, and artifact checksums are recorded in the release manifest.

B. Dataset-Driven Output Schema and Prompt

Each PlotChain item specifies an ordered set of expected output fields, partitioned into *final* fields and *checkpoint* fields. Checkpoint fields (prefixed `cp_`) are intermediate reads intended to diagnose where failures occur (e.g., reading a cutoff frequency correctly but computing a derived quantity incorrectly). The evaluator constructs a strict JSON schema *per item* from the dataset metadata and instructs the model to return *only* a single JSON object containing numeric values (or `null`) for those keys.

C. Robust Output Parsing

We enforce a strict interface (single JSON object), but we also implement robust extraction to ensure the benchmark measures plot-reading ability rather than brittle formatting

errors. Given the raw model response, the evaluator attempts: (i) direct JSON parsing, (ii) parsing a fenced ````json` block if present, and (iii) extracting the first `{ ... }` span. To mitigate a common real-world failure mode where models output arithmetic expressions (e.g., $1025/615$) despite instructions, the parser sanitizes simple fractions into decimal values and removes trailing commas before re-parsing. If parsing fails, all fields are treated as missing (equivalently `null`) for scoring.

D. Tolerance-Based Numeric Scoring

Let g denote the ground-truth numeric value for a field and p the model-predicted value. We compute absolute error $e_{\text{abs}} = |p - g|$ and relative error $e_{\text{rel}} = |p - g| / \max(|g|, \epsilon)$ with $\epsilon = 10^{-12}$. A prediction *passes* if it falls within either an absolute tolerance τ_{abs} or a relative tolerance τ_{rel} :

$$\text{PASS}(p, g) = \mathbb{I}[e_{\text{abs}} \leq \tau_{\text{abs}} \vee e_{\text{rel}} \leq \tau_{\text{rel}}]. \quad (1)$$

Tolerances are defined per (family, field) to reflect realistic human plot reading given axis resolution and visual affordances. We report all results under the *plotread* tolerance policy.

E. Metrics and Aggregation

We compute field-level, item-level, and model-level metrics, separating *final* fields from *checkpoint* fields:

- **Field pass rate:** mean of Eq. (1) over all items for a given (family, field).
- **Item final-pass:** an item passes if *all* final fields pass.
- **Item checkpoint-pass:** an item passes if *all* checkpoint fields pass.

- **Model final pass rate:** fraction of items that final-pass (headline metric).
- **Model checkpoint pass rate:** fraction of items that checkpoint-pass (diagnostic metric).
- **Error statistics:** mean absolute error and mean relative error computed over numeric fields (excluding missing values).
- **Latency:** per-call runtime as recorded by the evaluator.

In addition to aggregates, we persist the raw model outputs (`raw_{provider}_{model}.jsonl`) so that all metrics can be recomputed without additional API calls under alternative tolerance policies or parsing rules.

F. Paired Significance Testing

Because all models are evaluated on the *same fixed set of items*, comparisons between models are paired. For the headline *binary* metric (item strict all-pass over final fields), we use McNemar’s exact test on discordant item outcomes [27] and apply Holm correction across all pairwise comparisons [28]. We additionally report paired bootstrap 95% confidence intervals for the difference in strict all-pass rates (resampling items with replacement) [29]. For the *continuous* per-item metric (item final-field accuracy: mean of final-field pass indicators per item), we use paired *t*-tests and report Cohen’s *d* on paired differences [30], again with Holm correction across pairwise comparisons [28].

V. RESULTS

We report PlotChain results under the `plotread` tolerance policy (Sec. IV-D) with deterministic decoding (temperature = 0) and a strict numeric-JSON interface (Secs. IV-B–IV-C). Each model is evaluated on the same fixed set of 450 items (15 families \times 30 items). We report both: (i) *field-level pass rate* (fraction of individual numeric fields within tolerance), and (ii) *item-level strict all-pass* (an item passes only if *all* final fields for that item pass). Because each item typically contains multiple required numeric outputs, strict all-pass is a more discriminative (and more conservative) headline metric.

A. Overall performance and ranking

Table III summarizes overall performance. On the headline item-level strict all-pass metric, Gemini 2.5 Pro ranks first (72.0%), followed by GPT-4.1 (68.4%), Claude Sonnet 4.5 (61.3%), and GPT-4o (32.4%). Field-level pass rates are higher (as expected), with Gemini 2.5 Pro, GPT-4.1, and Claude Sonnet 4.5 clustered near ~78–80%, while GPT-4o is substantially lower.

B. Family-level performance

Figure 2 reports *family-level final-field pass rate* under `plotread`. Each cell aggregates pass/fail over the *final* (non-`cp_*`) numeric fields for all items in a plot family, providing a robust view of how often models recover the required end targets even when strict all-fields-per-item completion is not achieved.

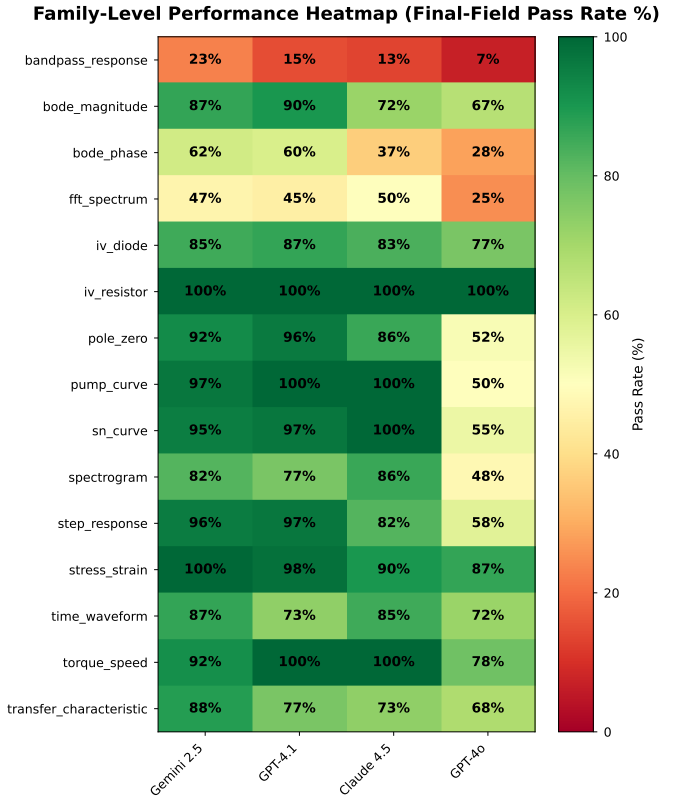


Fig. 2: Family-level performance heatmap (final-field pass rate, %). Each cell is the percentage of *final* (non-`cp_*`) fields that pass tolerance, aggregated over all items in the family.

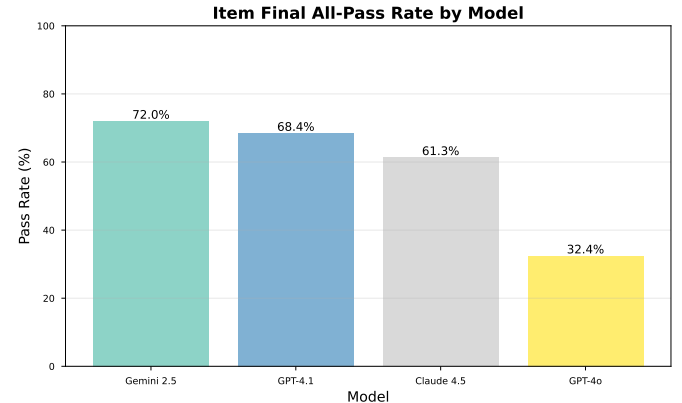


Fig. 3: Headline ranking by item-level strict all-pass (all final fields must pass).

Performance varies substantially across families. Several families are near-solved for frontier models, including I–V (RESISTOR) (100% for all models) and high-performing response families such as BODE MAGNITUDE (72–90%). In contrast, frequency-domain and derived-quantity families remain the dominant bottleneck: BANDPASS RESPONSE is consistently low (7–23% across models) and FFT SPECTRUM remains challenging (25–50%). These gaps indicate

TABLE III: Overall PlotChain results under `plotread` tolerances (temperature = 0). Field-level metrics are computed over all scored numeric fields. “Final-field acc.” is the per-item average accuracy over final (non-`cp_*`) fields. “Strict all-pass” is the fraction of items where *all final fields* pass.

Model	Field pass	Final-field pass	Checkpoint-field pass	Final-field acc.	Strict all-pass	Checkpoint all-pass [†]	Latency (s)
Gemini 2.5 Pro	80.4%	83.1%	76.5%	82.1%	72.0%	69.2%	20.66
GPT-4.1	79.8%	81.9%	76.9%	80.7%	68.4%	70.8%	1.97
Claude Sonnet 4.5	78.2%	77.7%	78.9%	77.1%	61.3%	75.4%	6.13
GPT-4o	61.6%	57.0%	68.3%	58.0%	32.4%	59.2%	2.22

[†]Checkpoint all-pass is computed over items that include at least one checkpoint field.

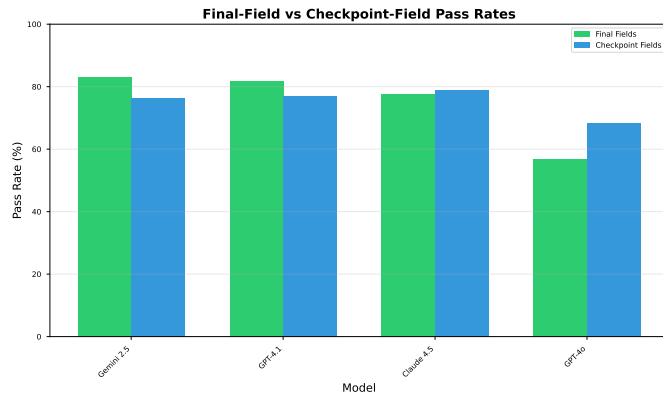


Fig. 4: Final vs. checkpoint field pass rates by model under `plotread`.

that quantitative extraction is not uniformly solved and that PlotChain retains diagnostic headroom across canonical engineering tasks.

C. Checkpoint diagnostics vs. final fields

Checkpoint fields (`cp_*`) are designed to localize failure causes by separating intermediate reads (e.g., crossing frequencies, peak locations) from final derived quantities. Figure 4 contrasts final vs. checkpoint field pass rates. Models differ systematically: GPT-4o and Claude Sonnet 4.5 tend to score relatively better on checkpoint fields than on final fields, consistent with extracting intermediate cues but failing to complete multi-step derivations reliably; Gemini 2.5 Pro and GPT-4.1 are comparatively stronger on final fields, suggesting fewer compounding errors from intermediate reads.

D. Paired model comparisons

Because all models are evaluated on the same fixed item set, comparisons are paired. For the headline strict all-pass metric (binary per item), we use McNemar’s exact test and report Holm-corrected p -values across all pairwise comparisons. Differences between the top three models are smaller than differences to GPT-4o; notably, Gemini 2.5 Pro vs. GPT-4.1 is not statistically significant at $\alpha = 0.05$ after correction, whereas GPT-4.1 and Gemini 2.5 Pro both significantly outperform Claude Sonnet 4.5, and all three significantly outperform GPT-4o.

TABLE IV: Paired comparisons on item-level strict all-pass (450 paired items). Δ is in percentage points (pp). McNemar uses exact binomial testing on discordant pairs, with Holm correction over all six pairwise tests.

Comparison	Δ (pp)	95% CI	p_{Holm}
Gemini 2.5 Pro vs GPT-4.1	+3.6	[-0.2, +7.3]	0.081
GPT-4.1 vs Claude Sonnet 4.5	+7.1	[+2.2, +11.8]	0.0044
Gemini 2.5 Pro vs Claude Sonnet 4.5	+10.7	[+6.4, +14.9]	3.8×10^{-6}
Claude Sonnet 4.5 vs GPT-4o	+28.9	[+24.0, +33.6]	2.7×10^{-27}
GPT-4.1 vs GPT-4o	+36.0	[+31.1, +40.9]	3.1×10^{-39}
Gemini 2.5 Pro vs GPT-4o	+39.6	[+35.1, +44.2]	3.4×10^{-45}

VI. DISCUSSION

PlotChain is designed to diagnose *plot-reading* rather than OCR-only transcription or generic captioning: models must infer quantitative values from axes, scales, and visual structure, and often combine multiple intermediate reads into derived quantities. The results show three main takeaways.

A. Frontier models cluster on field-level accuracy, but diverge on strict end-to-end completion

At the field level, Gemini 2.5 Pro, GPT-4.1, and Claude Sonnet 4.5 cluster around $\sim 78\text{--}80\%$ pass rates (Table III), indicating that all three can often recover individual numeric targets from plots under human-realistic tolerances. However, the item-level strict all-pass metric amplifies compounding errors: requiring *all* final fields for an item to be correct reduces headline performance, with Gemini 2.5 Pro at 72.0% and GPT-4.1 at 68.4% (Table III). Paired comparisons on strict all-pass confirm that the top-two gap is modest (Table IV), while differences versus GPT-4o are substantial. This illustrates why deterministic, multi-field items are valuable: they test reliable end-to-end completion rather than isolated “some numbers right” behavior.

B. Bottlenecks concentrate in derived-quantity families

Performance is highly family-dependent (Fig. 2). Families that require reading multiple crossings or peaks and then computing a derived parameter remain challenging. For example, BANDPASS RESPONSE is unsolved under strict all-pass in our setting (0% across models), even though models sometimes recover individual intermediate values within tolerance. This pattern is consistent with a *compounding-error* regime: small

read errors in two or more dependent measurements (e.g., f_1 and f_2 at -3 dB) can invalidate the derived bandwidth or Q under strict all-pass. In contrast, families with a single dominant readout or a clearer geometric structure (e.g., I–V (RESISTOR)) can be near-solved.

C. Checkpoint fields localize failure modes beyond headline accuracy

Checkpoint fields (`cp_*`) were introduced to distinguish failures in *reading* the plot from failures in *propagating* that read into downstream values. Figure 4 shows that checkpoint vs. final field pass rates differ across models: some models extract intermediate cues more reliably than they finish multi-step derivations. This enables actionable diagnostics: if a model passes checkpoints but fails finals, improvements should focus on arithmetic/derivation robustness and constraint following; if a model fails checkpoints, the bottleneck is upstream perception and axis calibration. We view checkpoint-based scoring as complementary to conventional final-answer evaluation, and especially useful for tracking progress on specific failure sources as models evolve.

D. Accuracy–latency tradeoffs matter for practical evaluation

Our runs exhibit a clear accuracy–latency tradeoff (Table III). GPT-4.1 achieves competitive item-level strict all-pass with low latency (1.97 s), while Gemini 2.5 Pro attains the highest strict all-pass at substantially higher latency (20.66 s). Claude Sonnet 4.5 occupies an intermediate point (6.13 s), and GPT-4o is fast but substantially less accurate (2.22 s). Such tradeoffs matter for practical engineering workflows where throughput and cost constraints can be as important as marginal gains in accuracy.

VII. LIMITATIONS AND THREATS TO VALIDITY

A. Synthetic plots and coverage

PlotChain uses a deterministic generator to produce “gold” ground truth from known parameters. This enables exact scoring and reproducibility, but synthetic plots may not capture all artifacts found in real lab/field plots (e.g., camera noise, compression, inconsistent styling, handwritten annotations, or overprinted legends). We mitigate this by including multiple families, difficulty tiers, and edge-case renderings, but additional real-world evaluation remains future work.

B. Tolerance dependence

Our primary metric uses per-family/per-field tolerances intended to reflect realistic human plot reading. While this makes evaluation more faithful to the task, rankings can shift under different tolerance policies, especially for borderline reads near resolution limits. To reduce ambiguity, we publish the tolerance policy, report both field- and strict item-level metrics, and release raw outputs to enable re-scoring without additional API calls.

C. Interface constraints and compliance

We require a strict numeric-JSON output schema to enable automated scoring. This is necessary for reproducibility, but it can penalize otherwise-correct reasoning if a model violates the interface (e.g., invalid JSON). We partially address this via robust parsing and by retaining raw outputs for audit; nevertheless, strict all-pass reflects an end-to-end requirement that includes adherence to an evaluation contract.

D. Model and platform variability

Results reflect specific model versions and run configurations at the time of evaluation. Provider-side changes (model updates, serving stack changes, or safety filters) may affect outcomes. We record run dates, settings, and checksums, and we release scripts and artifacts so results can be reproduced under the same conditions when possible. To preserve double-blind review, we will release the generator, evaluation scripts, tolerance policy, and raw outputs publicly upon acceptance.

E. Scope of tasks

PlotChain emphasizes numeric extraction and derived-quantity computation from canonical engineering plots. It does not directly test open-ended explanation quality, textual reasoning over captions, or tasks requiring domain-specific external knowledge beyond what is visible in the figure. These are complementary capabilities and can be evaluated with other benchmarks alongside PlotChain.

VIII. CONCLUSION

We introduced PlotChain, a deterministic, generator-based benchmark for evaluating multimodal LLMs on quantitative engineering plot reading. Unlike OCR-only or captioning-style evaluations, PlotChain pairs rendered plots with exact ground truth computed from generation parameters and augments final numeric targets with `cp_*` checkpoint fields that expose intermediate reads for diagnostic analysis. The benchmark spans 15 canonical plot families (450 items total) with controlled difficulty and edge cases, enabling reproducible, fine-grained capability profiling across models.

Across four state-of-practice multimodal LLMs, we find that frontier models cluster on field-level pass rates, but diverge under strict end-to-end completion when multiple dependent outputs must be simultaneously correct. Family-level analyses reveal persistent bottlenecks in derived-quantity settings (e.g., frequency-response and spectrum-based tasks), while checkpoint metrics help distinguish upstream perception/axis-calibration failures from downstream derivation or error-compounding failures. Paired statistical comparisons confirm that the two top models in our study are statistically indistinguishable under `plotread` after multiple-comparison correction, while all three frontier models substantially outperform GPT-4o.

PlotChain and its evaluation artifacts are released to support transparent, repeatable benchmarking and to enable re-scoring under alternative tolerance policies without additional model queries. We hope PlotChain serves as a practical diagnostic

tool for tracking progress in quantitative visual reasoning on engineering plots, and as a foundation for future extensions to broader plot styles, additional real-world noise sources, and new diagnostic families.

REFERENCES

- [1] S. E. Kahou, V. Michalski, A. Atkinson, Á. Kádár, A. Trischler, and Y. Bengio, “Figureqa: An annotated figure dataset for visual reasoning,” *arXiv preprint arXiv:1710.07300*, 2017. [Online]. Available: <https://arxiv.org/abs/1710.07300>
- [2] K. Kafle, B. L. Price, S. Cohen, and C. Kanan, “Dvqa: Understanding data visualizations via question answering,” in *Proceedings of the IEEE/CVF Conference on Computer Vision and Pattern Recognition (CVPR)*, 2018, pp. 5648–5656. [Online]. Available: https://openaccess.thecvf.com/content_cvpr_2018/papers/Kafle_DVQA_Understanding_Data_CVPR_2018_paper.pdf
- [3] N. Methani, P. Ganguly, M. M. Khapra, and P. Kumar, “Plotqa: Reasoning over scientific plots,” in *Proceedings of the IEEE Winter Conference on Applications of Computer Vision (WACV)*, 2020, pp. 1516–1525. [Online]. Available: https://openaccess.thecvf.com/content_WACV_2020/papers/Methani_PlotQA_Reasoning_over_Scientific_Plots_WACV_2020_paper.pdf
- [4] A. Masry, D. X. Long, J. Q. Tan, S. R. Joty, and E. Hoque, “A benchmark for question answering about charts with visual and logical reasoning,” in *Findings of the Association for Computational Linguistics: ACL 2022*, 2022. [Online]. Available: <https://aclanthology.org/2022.findings-acl.177/>
- [5] Xu *et al.*, “Chartbench: A benchmark for multimodal chart understanding,” *arXiv preprint arXiv:2312.15915*, 2023. [Online]. Available: <https://arxiv.org/abs/2312.15915>
- [6] P. Lu, H. Bansal, T. Xia, J. Liu, C. Li, H. Hajishirzi, H. Cheng, K.-W. Chang, M. Galley, and J. Gao, “Mathvista: Evaluating mathematical reasoning of foundation models in visual contexts,” in *International Conference on Learning Representations (ICLR)*, 2024. [Online]. Available: <https://arxiv.org/abs/2310.02255>
- [7] X. Yue *et al.*, “MMMU: A massive multi-discipline multimodal understanding and reasoning benchmark,” in *Proceedings of the IEEE/CVF Conference on Computer Vision and Pattern Recognition (CVPR)*, 2024. [Online]. Available: <https://arxiv.org/abs/2311.16502>
- [8] J. Pineau, P. Vincent-Lamarre, K. Sinha, V. Larivière, A. Beygelzimer, F. d’Alché Buc, E. Fox, and H. Larochelle, “Improving reproducibility in machine learning research (a report from the neurips 2019 reproducibility program),” *Journal of Machine Learning Research*, vol. 22, no. 164, pp. 1–20, 2021. [Online]. Available: <https://jmlr.org/papers/volume22/20-303/20-303.pdf>
- [9] P. Liang, R. Bommasani, T. Lee, D. Tsipras *et al.*, “Holistic evaluation of language models,” *arXiv preprint arXiv:2211.09110*, 2022. [Online]. Available: <https://arxiv.org/abs/2211.09110>
- [10] D. H. Kim, E. Hoque, and M. Agrawala, “Answering questions about charts and generating visual explanations,” in *Proceedings of the 2020 CHI Conference on Human Factors in Computing Systems (CHI ’20)*, 2020. [Online]. Available: <https://dl.acm.org/doi/10.1145/3313831.3376467>
- [11] D. Jung, W. Kim, H. Song, J.-i. Hwang, B. Kim, and J. Seo, “Chartsense: Interactive data extraction from chart images,” in *Proceedings of the 2017 CHI Conference on Human Factors in Computing Systems (CHI ’17)*, 2017, pp. 6706–6717. [Online]. Available: <https://dl.acm.org/doi/10.1145/3025453.3025957>
- [12] N. Siegel, S. Kornblith, T. Chen, C. Castillo, L. Bourdev, S. Gupta, R. Girshick, and A. Farhadi, “Figureseer: Parsing result-figures in research papers,” in *European Conference on Computer Vision (ECCV) Workshops*, 2016. [Online]. Available: <https://ai2-website.s3.amazonaws.com/publications/Siegel16eccv.pdf>
- [13] J. Luo, Z. Li, J. Wang, and C.-Y. Lin, “Chartocr: Data extraction from charts images via a deep hybrid framework,” in *Proceedings of the IEEE Winter Conference on Applications of Computer Vision (WACV)*, 2021. [Online]. Available: https://openaccess.thecvf.com/content/WACV2021/papers/Luo_ChartOCR_Data_Extraction_From_Charts_Images_via_a_Deep_Hybrid_WACV_2021_paper.pdf
- [14] Z.-Q. Cheng, S. Zhu, C. Sun, D. Li, J. Luo, and J. Liu, “Chartreader: A unified framework for chart derendering and comprehension without manual rule-making,” in *Proceedings of the IEEE/CVF International Conference on Computer Vision (ICCV)*, 2023. [Online]. Available: https://openaccess.thecvf.com/content/ICCV2023/papers/Cheng_ChartReader_A_Unified_Framework_for_Chart_Derendering_and_Comprehension_without_ICCV_2023_paper.pdf
- [15] K. Lee, M. Joshi, I. Turc, H. Hu, F. Liu, J. Eisenschlos *et al.*, “Pix2struct: Screenshot parsing as pretraining for visual language understanding,” in *Proceedings of the 40th International Conference on Machine Learning (ICML)*, 2023. [Online]. Available: <https://arxiv.org/abs/2210.03347>
- [16] A. Masry, P. Kavehzadeh, J. Q. Tan, S. R. Joty, and E. Hoque, “Unichart: A universal vision-language pretrained model for chart comprehension and reasoning,” in *Proceedings of the 2023 Conference on Empirical Methods in Natural Language Processing (EMNLP)*, 2023. [Online]. Available: <https://aclanthology.org/2023.emnlp-main.906/>
- [17] F. Liu, F. Piccinno, S. Krichene, J. Eisenschlos *et al.*, “Deplot: One-shot visual language reasoning by plot-to-table translation,” in *Findings of the Association for Computational Linguistics: ACL 2023*, 2023. [Online]. Available: <https://arxiv.org/abs/2212.10505>
- [18] K.-H. Huang *et al.*, “Do l1lms understand charts? analyzing and correcting chart reasoning failures,” *Findings of the Association for Computational Linguistics: ACL 2024*, 2024. [Online]. Available: <https://aclanthology.org/2024.findings-acl.41/>
- [19] J. Obeid and E. Hoque, “Chart-to-text: Generating natural language descriptions for charts by adapting the transformer model,” in *Proceedings of the 13th International Conference on Natural Language Generation (INLG)*, 2020. [Online]. Available: <https://aclanthology.org/2020.inlg-1.20/>
- [20] S. Kantharaj, A. Masry, S. R. Joty, E. Hoque *et al.*, “A large-scale benchmark for chart summarization,” in *Proceedings of the 60th Annual Meeting of the Association for Computational Linguistics (ACL)*, 2022. [Online]. Available: <https://aclanthology.org/2022.acl-long.277/>
- [21] Xia *et al.*, “Chartx & chartvlm: A versatile benchmark and foundation model for chart understanding,” *arXiv preprint arXiv:2402.12185*, 2024. [Online]. Available: <https://arxiv.org/abs/2402.12185>
- [22] Y. Liu, H. Duan, Y. Huang, J. Wang *et al.*, “Mmbench: Is your multi-modal model an all-around player?” in *European Conference on Computer Vision (ECCV)*, 2024. [Online]. Available: <https://arxiv.org/abs/2307.06281>
- [23] M. Ravishankara and V. V. Persad Maharaj, “The artificial intelligence cognitive examination: A survey on the evolution of multimodal evaluation from recognition to reasoning,” *IEEE Access*, pp. 1–1, 2025.
- [24] P. Virtanen, R. Gommers, T. E. Oliphant, M. Haberland, T. Reddy, D. Cournapeau, E. Burovski, P. Peterson, W. Weckesser, J. Bright, S. J. van der Walt, M. Brett, J. Wilson, K. J. Millman, N. Mayorov, A. R. J. Nelson, E. Jones, R. Kern, E. Larson, C. J. Carey, I. Polat, Y. Feng, E. W. Moore, J. VanderPlas, D. Laxalde, J. Perktold, R. Cimrman, I. Henriksen, E. A. Quintero, C. R. Harris, A. M. Archibald, A. H. Ribeiro, F. Pedregosa, and P. van Mulbregt, “SciPy 1.0: Fundamental algorithms for scientific computing in Python,” *Nature Methods*, vol. 17, no. 3, pp. 261–272, 2020. [Online]. Available: <https://www.nature.com/articles/s41592-019-0686-2>
- [25] C. R. Harris, K. J. Millman, S. J. van der Walt, R. Gommers, P. Virtanen, D. Cournapeau, E. Wieser, J. Taylor, S. Berg, N. J. Smith, R. Kern, M. Picus, S. Hoyer, M. H. van Kerkwijk, M. Brett, A. Haldane, J. F. del Río, M. Wiebe, P. Peterson, P. Gérard-Marchant, K. Sheppard, T. Reddy, W. Weckesser, H. Abbasi, C. Gohlke, and T. E. Oliphant, “Array programming with NumPy,” *Nature*, vol. 585, no. 7825, pp. 357–362, 2020. [Online]. Available: <https://arxiv.org/abs/2006.10256>
- [26] J. D. Hunter, “Matplotlib: A 2d graphics environment,” *Computing in Science & Engineering*, vol. 9, no. 3, pp. 90–95, 2007.
- [27] Q. McNemar, “Note on the sampling error of the difference between correlated proportions or percentages,” *Psychometrika*, vol. 12, no. 2, pp. 153–157, 1947.
- [28] S. Holm, “A simple sequentially rejective multiple test procedure,” *Scandinavian Journal of Statistics*, vol. 6, no. 2, pp. 65–70, 1979.
- [29] B. Efron and R. J. Tibshirani, *An Introduction to the Bootstrap*. Chapman and Hall/CRC, 1993.
- [30] J. Cohen, *Statistical Power Analysis for the Behavioral Sciences*, 2nd ed. Lawrence Erlbaum Associates, 1988.